# Experimental Study on the Relationship between Attenuation Coefficient and Data Rate in Free Space Optical Communication

**Ibukunoluwa Adetutu Olajide**
Department of Electrical and Electronics Engineering
The Federal University of Technology
Akure, Nigeria
iaadebanjo@futa.edu.ng

**Samson Adenle Oyetunji**
Department of Electrical and Electronics Engineering
The Federal University of Technology
Akure, Nigeria
saoyetunji@futa.edu.ng

*Abstract*—**This study explores the dynamics of optical power transmission and reception in Free Space Optical (FSO) communication systems, focusing on the relationship between the attenuation coefficient, data rate, and propagation distance. Utilizing the Beer-Lambert law as a foundational premise, we investigated how variations in these parameters influence the efficiency and reliability of FSO links. Through analytical and graphical analysis, we delineated the effects of data rate on transmittance and optical power loss across three wavelengths (808 nm, 980 nm, and 1550 nm). The study further introduces novel mathematical models derived from curve fitting optimization techniques to predict the impact of data rate changes on the attenuation coefficient. The findings offer critical insights into the design and optimization of optical communication systems, emphasizing the need for wavelength-specific considerations to manage signal degradation effectively.**

*Keywords—Attenuation coefficient, Data rate, Optical Power Loss, Transmittance.*

## I. INTRODUCTION

Free Space Optical Communication (FSO) stands as a cutting-edge technology facilitating the transmission of information, including voice, video, and text, through optical radiation in the free space medium, predominantly the Earth's atmosphere [1] [2]. Originating from the escalating demand for high-speed and secure communication systems, FSO emerged as a promising solution [3]. This communication technique exhibits notable advantages in addressing challenges related to losses, security concerns, central connectivity, spectrum utilization, and bandwidth management. FSO systems deploy line-of-sight technology, predominantly utilizing laser beams for transmission [4]. Categorically, FSO communication systems can be classified into terrestrial and space optical links. Space optical links encompass ground-to-satellite/satellite-to-ground links, inter-satellite links, and deep space links. In contrast, terrestrial setups, typically designed for short-range communication, are established between buildings [5]-[7].

Free Space Optical Communication (FSO) has emerged as a compelling alternative to address the challenges of broadband connectivity, particularly in solving the 'Last Mile' problem. In comparison to Radio Frequency (RF) and Millimeter Wave technologies, which face limitations such as spectrum congestion, licensing issues, and interference, FSO stands out as a promising solution for wireless communication, overcoming these hurdles [8], [2], [6]. RF and Millimeter Wave technologies, while offering data rates from tens to several hundreds of megabits per second, are constrained by spectrum congestion, license complications, and interference from adjacent bands. FSO, positioned as a substitute for the last and first mile problems, holds a distinct advantage due to its bandwidth capabilities, unencumbered by the limitations faced by RF technologies [6].

FSO's superiority is further underscored by the velocity of light transfer, as light travels faster through air than in traditional mediums such as glass-fiber [9]. Additionally, FSO boasts of a significant wavelength difference compared to RF and Millimeter Wave technologies, operating in the near-Infrared (IR) region with a wavelength window between 700 and 1600 mm [5]. This large wavelength difference contributes to FSO's substantial bandwidth advantage over RF technology, with an optical carrier frequency ranging from $10^{12}$ to $10^{16}$ Hz [6]. The narrow beam size of FSO, utilizing laser beams with a diffraction unit of approximately 0.1 mrad, enhances its resilience to external influences and electromagnetic interference. This feature ensures a concentrated signal intensity at the receiver, making the FSO system reusable, secure, and robust [10].

With these enumerated advantages, this paper investigates experimentally three wavelength windows used in FSO; their optical supremacy and preferences in data transmission. The wavelength windows employed are 808 nm, 980 nm, and 1550 nm. Furthermore, a novel relationship was established between data rate and attenuation coefficients of the wavelength windows examined. The paper examines a connection between attenuation change and change in data rate. The paper is organized as follows: literature review is presented in Section II, the methodological
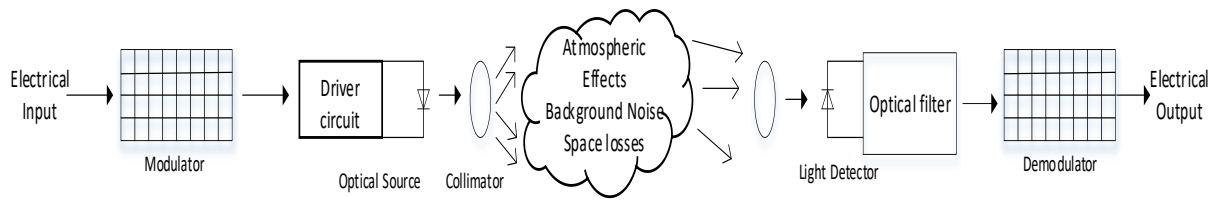
Fig. 1. : The basic setup of FSO system[11]

approach is provided in Section III, while the graphical analysis and discussion is given in Section IV. The conclusion is drawn in Section V.

## II. LITERATURE REVIEW

### A. Overview of Free Space Optical (FSO) Communication System

The Free Space Optical communication (FSO) system comprises three fundamental subsystems: the transmitter, the channel, and the receiver[11]. The basic diagram is given in Fig.1.

#### 1) Transmitter

As depicted in Fig. 1, the transmitter subsystem of FSO is composed of multiple components, including an optical source, a modulator, a driver circuit, and lenses. The data may undergo encoding prior to modulation. Subsequently, the modulated data is transformed into an optical signal by the driver circuit[12]. The lenses are responsible for collecting and refocusing the light beams. Intensity Modulation (IM) is the most commonly employed modulation technique in FSO systems, where the data is modulated based on the intensity of optical radiation. This modulation can be implemented in two primary ways: firstly, by varying the driving current of the optical source in direct correlation with the transmitted data; secondly, through the utilization of an external modulator, such as the Mach-Zehnder modulator [6]. In the context of FSO, the optical source is typically either a Laser Diode (LD) or a high-power Light Emitting Diode (LED) equipped with beam collimators [10].

The optical source should ideally maintain optimal performance at high optical power across a broad temperature range. Additionally, it should possess a high Mean Time Between Failures (MTBF), compact size, and low power consumption [13]. There are primarily four types of lasers used in FSO systems: Vertical-Cavity Surface Emitting Laser (VCSEL), Fabry-Perot Laser, Distributed-feedback Laser, and Quantum Cascade Lasers [6], [10]. The selection of a particular laser type is influenced by factors such as safety standards and cost considerations. FSO systems generally operate within two spectral windows: 780-850nm and 1520-1600nm, with the former being more prevalent due to cost and availability [6]. The latter window is favored for its eye safety and the ability to transmit higher power, which is beneficial in mitigating the effects of fog. However, this window also

presents challenges, including reduced detector sensitivity, the necessity of expensive components, and the requirement for precise alignment at the receiver end [6].

#### 2) Channel

In the FSO system, the channel input signal is representative of power rather than amplitude, as detailed by [6]. Within the field of optical systems, the received electrical power is directly proportional to the square of the receiver area. Additionally, the variance of the shot noise is also proportional to the receiver area. This relationship implies that, for any given transmit power, a larger detector area will result in a higher Signal-to-Noise Ratio (SNR). The composition of the channel in FSO systems encompasses various elements such as gases, water vapor, and aerosols [6]. Moreover, the channel is subject to the influence of diverse and unpredictable environmental factors, including fog, rain, and snow. These environmental elements are in a state of constant flux, leading to turbulence and consequent attenuation of the received signal. This variability in environmental conditions plays a significant role in impacting the overall performance and reliability of the FSO system.

#### 3) Receiver

Light detectors are integral components within Free Space Optics (FSO) systems [9]. These receivers detect light through various phenomena. The fundamental architecture of an FSO system encompasses a receiver telescope, an optical pass filter, a photodetector, and a decision circuit [6]. The orchestration of these components plays a crucial role in the efficiency and effectiveness of light detection in FSO systems. Regarding the photodiodes utilized in FSO systems, two major types of solid-state photodiodes are predominantly used: the PIN photodiode and the Avalanche photodiode. A comprehensive literature review outlining the advantages and disadvantages of these photodiodes can be found in [10]. Additionally, other types of detectors used in FSO systems include photo-conductors and semiconductor metal photodiodes, as mentioned by [14]. These detectors play a pivotal role in the effective conversion of optical signals into electrical signals within the FSO framework.

## III. METHODOLOGY

### A. System Design

In order to appropriately carry out empirical analysis in optical communication, a transmitter and receiver units must be adequately designed. Fig. 2 shows the system setup for the empirical study.
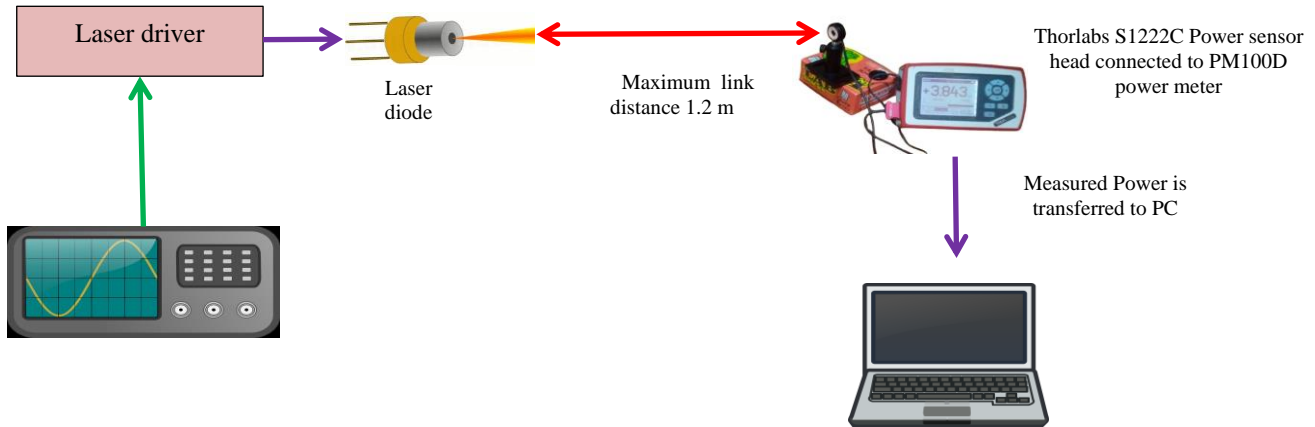


Fig. 2. : Schematic of the experimental setup

TABLE I. LASER DIODES SPECIFICATIONS

| Specification | Wavelengths | | |
|---|---|---|---|
| | *808 nm* | *980 nm* | *1550 nm* |
| Model Number | OPT808-500mW | ZRHF | L1550P5DFB |
| Laser Type | Continuous Wave | Continuous Wave | Continuous Wave |
| Output Power | 500 mW | 50 mW | 5 mW (Max. 10 mW) |
| Slope Efficiency | 0.8mW/mA | 0.8mW/mA | 0.24 W/A |
| Beam Divergence | 7° | - | 8° |

The data to be propagated was generated and sent to the laser driver using the Rigol Arbitrary Waveform Generator (AWG) DG2102; this data was sent through the propagating medium. Using the Non-Return to Zero coding, the data rate was varied from 2 kb/s to 20 Mb/s for the three wavelengths experimented with- 808nm, 980nm, and 1550nm. The laser specifications are given in Table 1.

In order to determine the relationship between data rate and attenuation coefficient, the data rate was varied proportionally with increase in distance. Due to high cost of FSO communication setup, the setup illustrated in Fig. 2 was set up in the laboratory under a controlled environment at room temperature in the dark. The distance was varied from 10 cm to 120 cm. The receiver is an optical power sensor connected to a power meter console. The Receiver is the S122C power head designed for general purpose optical power measurements made by Thorlabs. The head is optimized for small thickness to fit in tight spaces. The high sensitive photodiode with large active area in combination with an absorptive ND filter enables power measurements up to 50 mW in free space and fiber-based applications. A removeable annular VIS/IR viewing target allows conveniently centering the measured beam to the active area of the photo-diode. The target absorbs light from 400 to 640nm and 800 to 1700nm. The S122C sensor is connected to the PM100D power console for display of power measurements.

## IV. RESULTS AND DISCUSSION

### A. Transmittance

For FSO communication, the optical transmitted power is related to the optical received power through the Beer- Lambert law[15], given as

$$\tau(L) = \frac{P_r}{P_t} = e^{-\sigma L} \tag{1}$$

where $\tau$ is the transmittance at a distance L, $P_r$ is the received power (mW), $P_t$ is the transmit power (mW), $\sigma$ is the scattering/attenuation coefficient and L is the propagation distance.

In observing the relationship between transmittance and the attenuation coefficient equation (1) can further be expressed as :

$$\ln \tau(L) = -\sigma L \tag{2}$$

Equation (2) can further be expressed as :

$$\sigma = \frac{-\ln \tau(L)}{L} \tag{3}$$

Substituting for the transmittance in equation (3), the attenuation coefficient can further be expressed as:

$$\sigma = \frac{\ln \frac{P_t}{P_r}}{L} \tag{4}$$

Equation (4) implies that an inverse relationship exist between propagation distance and the

attenuation coefficient according to Beer Lambert's law. This inverse relationship indicates that any variations in the propagation distance or the attenuation coefficient will precipitate significant alterations in the counterpart parameter. However, it is critical to acknowledge that this formulation does not encompass modifications in the data transmission rate.

Further examination of the stated relationship, particularly when drawing parallels to the equation of a line, reveals that plotting the logarithm of the transmittance against the propagation distance yields a slope that corresponds to the negative value of the attenuation coefficient. This analytical approach facilitates a deeper comprehension of the attenuation phenomenon across different wavelengths (namely 808 nm, 980 nm, and 1550 nm) and varying data transmission rates, as demonstrated in the graphical representations provided in Fig. 3, 4, and 5.
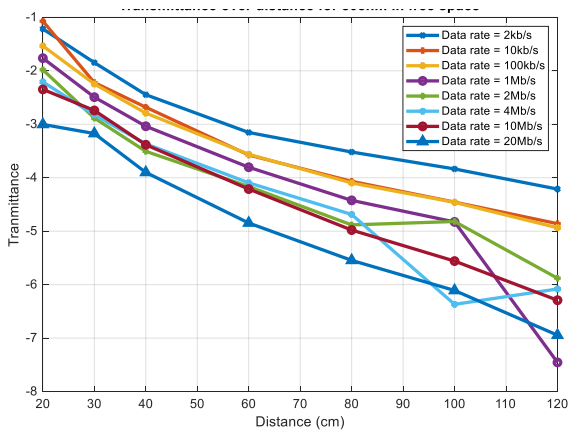


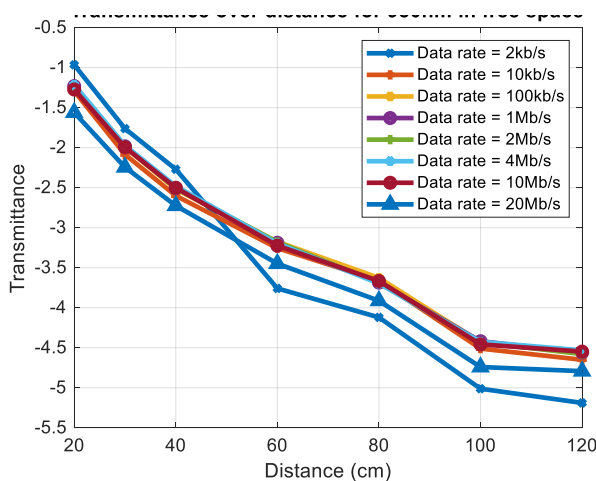Fig 3: Transmittance plot for varying distances for 808 nm



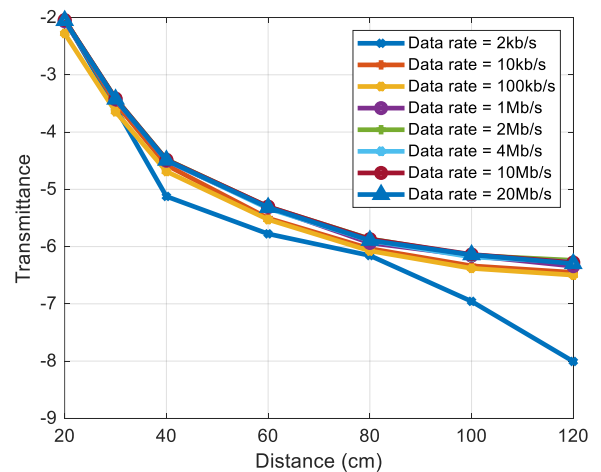Fig. 4: Transmittance plot for varying distances for 980 nm



Fig. 5: Transmittance plot for varying distances for 1550 nm

This comparative analysis underscores the fundamental principles underlying FSO communication and accentuates the pivotal role of the Beer-Lambert Law in elucidating the optical power transmission-reception dynamics.

Transmittance is a measure of how much of the original signal reaches the destination after a certain distance. As observed in Fig. 3, transmittance reduces as link distance increases. The data rate with the highest gradient is 2kb/s while 20Mb/s has the lowest gradient. The transmittance values presented in Fig. 4 for 980 nm shows a downward slope as propagation distance increases. Transmittance values of all data rates lied between -1 and -1.5. Experimented data rates between 10 kb/s and 10 Mb/s lie within the same boundary as observed, thereby indicating a better performance than that obtained at lower wavelength, 808 nm. The plot of transmittance over the propagation distance for selected data rates at 1550 nm wavelength is shown in Fig. 5. Transmittance reduces for all the data rate as propagation distance increased. Longer distances mean lower transmittance. The data rate of 2 kb/s has the lowest transmittance value compared to the other data rates; 10 kb/s and 100 kb/s data rates, which fall within the same transmittance values, appearing next to the 2 kb/s plot. Higher data rates give higher transmittance values. Compared to 808 nm and 980 nm wavelengths, the transmittance plot of 1550 nm gave a better transmittance against distance outlook.

### B. Free Space Optical Loss

In optical communication systems design, the quantification of optical power loss emerges as a critical parameter. This metric is derived by calculating the discrepancy between the transmitted and received optical powers, with consideration given to all conceivable losses encountered during the transmission process. Figs. 6, 7,and 8 shows the cumulative optical loss across three distinct wavelengths for a spectrum of data rates.

An analysis of Fig. 6 reveals that the data rate of 20 Mb/s exhibits the lowest optical power loss ratio,

whereas a rate of 2 kb/s incurs the highest ratio of power loss. Data rates spanning 100 kb/s, 1 Mb/s, and 2 Mb/s are characterized by comparably narrow variations in their optical power loss ratios. This observation facilitates an evaluation of the optimal data rate for minimizing power loss during transmission at an 808 nm wavelength, indicating a tendency towards lower optical power losses at higher data rates over various distances.

Conversely, for the 980 nm wavelength, as illustrated in Fig. 7, an increase in propagation distance is associated with a decrement in optical power loss across all data rates, a trend that contrasts with the behavior observed at the 808 nm wavelength. The data rates ranging from 10 kb/s to 4 Mb/s exhibit losses within a confined range on the plot, with 100 kb/s, 1 Mb/s, and 2 Mb/s experiencing nearly identical losses. Notably, the loss ratio for 2 kb/s data rate between distances of 20 cm and 120 cm surpasses that of the 20 Mb/s rate, suggesting that the disparity in loss ratios between shorter and longer distances diminishes as the propagation distance and data rate increase.
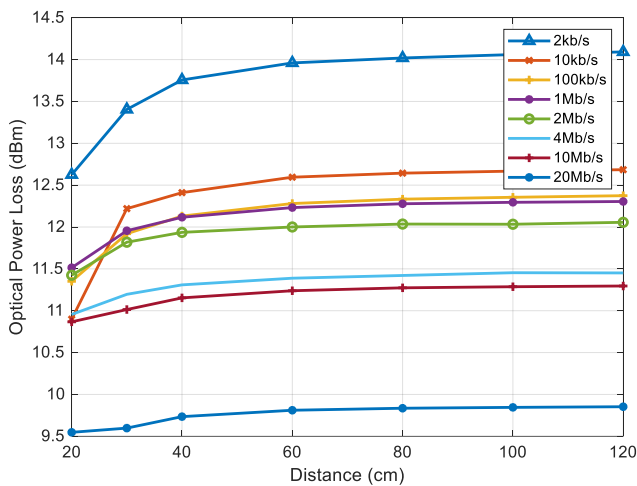


Fig. 6: Optical power loss across distances for 808 nm
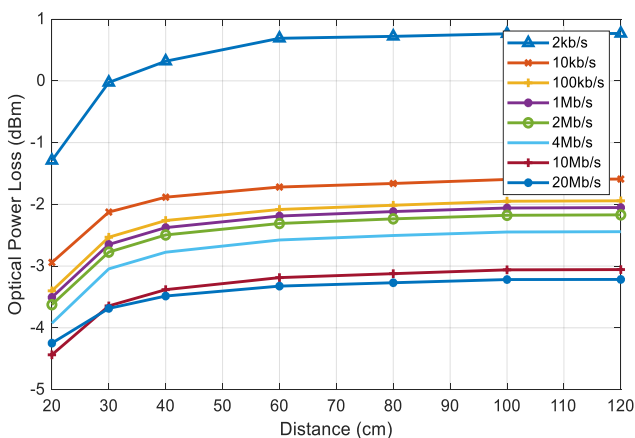


Fig. 7: Optical power loss across distances for (b) 980 nm
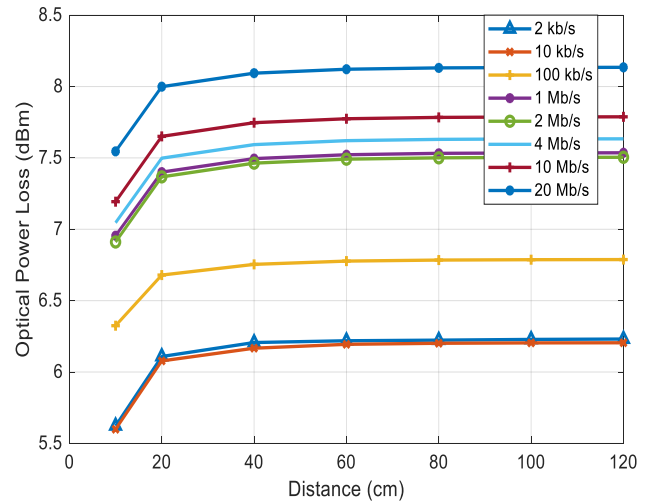


Fig. 8: Optical power loss across distances for 1550 nm.

In the case of the 1550 nm wavelength, as depicted in Fig. 8, an escalation in the distance between the transmitter and receiver (e.g., from 10 cm to 120 cm) directly correlates with an increase in signal loss. This phenomenon is attributed to the dispersion and attenuation of the signal over extended distances. Furthermore, at each given propagation distance, the optical signal loss for varying data rates (ranging from 2 kb/s to 20 Mb/s) remains relatively uniform. This indicates that while higher data rates may necessitate increased power output, the impact on optical signal loss is not significantly exacerbated. Additionally, the consistency in the pattern of signal loss across different data rates implies that the influence of factors such as absorption and scattering on signal loss is potentially minimized when employing the 1550 nm wavelength.

*C. The Attenuation Coefficient -Data rate relationship*

In a detailed plot presented in Fig. 9, the attenuation coefficients (measured in dB/m) for transmission links operating at wavelengths of 808 nm, 980 nm, and 1550 nm are analyzed in relation to various data rates. This analysis yields insightful observations regarding the interplay between data rate and optical signal attenuation across these wavelengths. For the 808 nm wavelength, a direct correlation is observed between the data rate and the attenuation coefficient. Specifically, as the data rate increases, there is a corresponding increase in the attenuation coefficient. This relationship suggests that, at an 808 nm wavelength, higher data rates are associated with greater attenuation coefficients, implying that the optical signal's integrity may be more susceptible to degradation as the data transmission rate increases, with potential reciprocal effects due to atmospheric conditions.
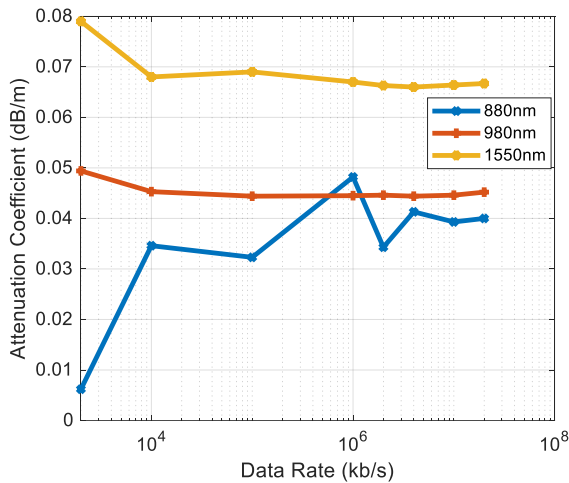
Fig. 9: Attenuation coefficient plot for varying distances in free space for 880nm, 980nm and 1550 nm.

Conversely, at the 980 nm wavelength, the attenuation coefficient's behavior is examined over various propagation distances for each data rate. It is noticed that the attenuation coefficient diminishes as the data rate increases. This trend indicates that for the 980 nm wavelength, higher data rates may be advantageous in terms of reducing the optical signal's attenuation, thereby potentially enhancing the efficiency and reliability of the transmission link over given distances.

The analysis extends to the 1550 nm wavelength, where the dependence of the attenuation coefficient on the data rate is further clarified. It is observed that the attenuation coefficient decreases with an increase in data rate. This phenomenon underscores a crucial aspect of optical communication design at the 1550 nm wavelength, where higher data rates appear to mitigate the attenuation effect, thereby suggesting a more stable and robust transmission capability under increased data loads.

These findings collectively provide a comprehensive understanding of how data rate influences optical signal attenuation across different wavelengths. They highlight the wavelength-specific considerations that must be accounted for in the design and optimization of optical communication systems to achieve desired performance metrics while managing signal degradation effects.

In addressing the limitation of Equation (4), which did not express the relationship between the attenuation coefficient and changes in data rate, a methodological approach was undertaken using curve fitting optimization techniques in MATLAB. This optimization technique, specifically chosen without the application of a robust fit method, aimed to precisely model the relationship between the attenuation coefficient and the propagation distance across all examined wavelengths. The objective was to generate a regression curve that could explain this relationship. From the regression analysis, a novel power equation was derived. This equation encloses the discovered relationship between the attenuation coefficient and

data rate, offering a mathematical framework to predict how changes in data rate influence the attenuation coefficient. The formulation of such an equation is instrumental for optical communication systems design, providing a quantitative tool to assess and optimize the performance of optical links across varying data rates and wavelengths. The analytical derivation provided culminates in Equation (5), which offers a novel expression to expresses the relationship between the attenuation coefficient, $\sigma$, and propagation data rate, D, for optical transmission links. This equation is formally stated as:

$$\sigma_\lambda = \delta D^x$$

(5)

where $\sigma_\lambda$ is the attenuation coefficient (in dB/m) for λ wavelength, D is the propagation data rate (in b/s) and d is a wavelength-dependent variable (in s/m). This equation introduces a power-law relationship between the attenuation coefficient and the data rate, with δ and x as parameters that adjust the equation to fit specific wavelength conditions.

For the 808 nm transmission link, the specific form of this equation is given as Equation (6), where the values of $d = 0.01896$ s/m and $x = 0.07515$ are tailored to this particular wavelength. This adaptation of Equation (5) to the 808 nm context provides a precise model for predicting how the attenuation coefficient varies with data rate at this wavelength.

$$\sigma_{808} = 0.01896D^{0.07515}$$

(6)

For the 980 nm transmission link, Equation (7) modifies the general form to suit the 980 nm wavelength.

$$\sigma_{980} = 0.04654D^{-0.002939}$$

(7)

where $\sigma_{980}$ is the attenuation coefficient (dB/m) for 980 nm wavelength, and D is the propagation data rate in (bits/s).

It is noted that an increase in the data rate results in a decrease in the attenuation coefficient. This relationship is characterized by a negative exponent for D, indicating an inverse exponential relationship between the data rate and attenuation for the 980 nm wavelength.

For 1550nm link, the descriptive equation for 1550nm link is given as

$$\sigma_{1550} = 0.0843D^{-0.01622}$$

(8)

where $\sigma_{1550}$ is the attenuation coefficient ( dB/m) for 1550 nm wavelength, and D is the propagation data rate (b/s) .

The equation represents a relationship where the attenuation coefficient decreases as data rate increases and considering the small magnitude of its exponential value x (i.e., -0.01622), it is suggestive that the effect of the data rate on attenuation is relatively weak.

## V. CONCLUSION

This study advances the understanding of FSO communication by highlighting the critical role of data rate and propagation distance in influencing the attenuation coefficient. The novel mathematical models introduced for predicting the impact of data rate changes on attenuation provide a significant contribution to the field, offering a quantitative basis for the design and optimization of optical communication systems. Future work will focus on extending this analysis to include atmospheric conditions, aiming to develop comprehensive models that encompass all factors affecting FSO communication efficiency.

REFERENCES

[1] R. Hou, Y. Chen, J. Wu, and H. Zhang."A brief survey of optical wireless communication". In Proc. of the 13th Australasian Symposium on Parallel and Distributed Computing, vol. 2730, pp. 41-50, 2015.

[2] A. Malik, and P. Singh. "Free space optics: current applications and future challenges". International Journal of Optics, Hindawi Publishing Corporation, 2015.

[3] H. Henniger, and O. Wilfert. "An Introduction to Free-space Optical Communications". RadioEngineering, vol.19 no 2, 2010.

[4] M. A. Khalighi, and M. Uysal. "Survey on free space optical communication: A communication theory perspective". IEEE Communications Surveys & Tutorials, vol. 16 no 4, pp. 2231-2258, 2014.

[5] H. Kaushal, and G.Kaddoum. "Optical communication in space: Challenges and mitigation techniques". IEEE communications surveys & tutorials, vol.19 no.1, pp. 57-96, 2017.

[6] Z. Ghassemlooy, and W. O. Popoola. "Terrestrial free-space optical communications", InTech, 2010, pp. 355-392.

[7] G. Y. Hu, C .Y. Chen, and Z. Q. Chen. "Free-space optical communication using visible light". Journal of Zhejiang University-SCIENCE A, vol. 8, no.2, pp. 186-191,2007.

[8] A. K. Majumdar. "Advanced Free Space Optics (FSO): A Systems Approach", Springer series in Optical science, vol. 186, New York, 2014.

[9] H. Willebrand, and B. S. Ghuman. Free space optics: enabling optical connectivity in today's networks. SAMS publishing, Indiana, 2002.

[10] M.A. Khalighi, and M. Uysal. "Survey on free space optical communication: A communication theory perspective". IEEE Communications Surveys & Tutorials, vol. 16 no 4, pp. 2231-2258, 2014.

[11] J. Li, J. Q. Liu, and D. P. Taylor. "Optical communication using subcarrier PSK intensity modulation through atmospheric turbulence channels". IEEE Transactions on Communications, vol. 55 no. 8, pp. 1598-1606, 2007.

[12] A. G. Alkholidi, and K. S. Altowij. "Free space optical communications—Theory and practices", In Contemporary Issues in Wireless Communications. InTech, 2014.

[13] S. Bloom, E. Korevaar, J. Schuster, and H. Willebrand. "Understanding the performance of free-space optics". Journal of optical Networking, vol. 2 no. 6, pp. 178-200, 2003.

[14] Z. Ghassemlooy, W. Popoola, and S. Rajbhandari, Optical wireless communications: system and channel modelling with Matlab®. CRC press, 2012, pp. 66-72

[15] Report ITU-R F.2106–1, "Fixed service applications using free-space optical links". https://www.itu.int/pub/R-REP-F.2106-2007, 2011